Eur. Phys. J. A **39**, 33–48 (2009)
DOI 10.1140/epja/i2008-10693-3

THE EUROPEAN PHYSICAL JOURNAL A

Regular Article – Experimental Physics

Nuclear structure of ^{189}Tl states studied via β^+/EC decay and laser spectroscopy of $^{189m+g}$Pb

J. Sauvage[1,a], J. Genevey[2], B. Roussière[1], S. Franchoo[1,3,4], A.N. Andreyev[5,6,7], N. Barré[1], J.-F. Clavelin[1], H. De Witte[5], D.V. Fedorov[8], V.N. Fedoseyev[4], L.M. Fraile[4,b], X. Grave[1], G. Huber[3], M. Huyse[5], H.B. Jeppesen[4,c], U. Köster[4,9], P. Kunz[3], S.R. Lesher[5,d], B.A. Marsh[4], I. Mukha[5,e], J. Oms[1], M. Seliverstov[3,8], I. Stefanescu[5,f], K. Van de Vel[5,g], J. Van de Walle[4], P. Van Duppen[5], and Yu.M. Volkov[8]

[1] Institut de Physique Nucléaire, IN2P3-CNRS/Université Paris-Sud, F-91406 Orsay Cedex, France
[2] Laboratoire de Physique Subatomique et de Cosmologie, IN2P3-CNRS/Université Joseph Fourier, F-38026 Grenoble Cedex, France
[3] Institut für Physik, Johannes Gutenberg Universität, D-55099 Mainz, Germany
[4] ISOLDE, CERN, CH-1211 Genève 23, Switzerland
[5] Instituut voor Kern- en Stralingsfysica, K.U. Leuven, B-3001 Leuven, Belgium
[6] Oliver Lodge Laboratory, University of Liverpool, Liverpool, L69 7ZE, UK
[7] TRIUMF, Vancouver BC, V6T 2A3, Canada
[8] Petersburg Nuclear Physics Institute, 188350, Gatchina, Russia
[9] Institut Laue-Langevin, 38042 Grenoble cedex 9, France

Received: 28 August 2008 / Revised: 13 November 2008
Published online: 14 January 2009 –
Communicated by J. Äystö

Abstract. The β^+/EC decay of ^{189m,g}Pb has been studied at the ISOLDE facility using nuclear spectroscopy and in-source laser spectroscopy. A level scheme of ^{189}Tl has been built from γ-γ coincidence relationships and information on the feeding of some excited levels of ^{189}Tl provided by the hyperfine spectra obtained from laser ionization. The half-lives of both the $13/2^+$ and $3/2^-$ ^{189}Pb isomers have been estimated to be $T_{1/2} = 50 \pm 3$ s and $T_{1/2} = 39 \pm 8$ s, respectively. Calculations have been performed for different oblate and prolate nuclear deformations using an axial-rotor coupled to one-quasiparticle model, a structure has been suggested for the low-lying levels of the ^{189}Tl nucleus.

PACS. 21.10.Hw Spin, parity, and isobaric spin – 23.20.Lv γ transitions and level energies – 42.62.Fi Laser spectroscopy – 21.60.Ev Collective models

1 Introduction

Large differences in nuclear shape for the isomeric and ground states of the neutron-deficient isotopes have been established from the change in the mean square charge radius deduced from isotope shift measurements along the thallium, mercury, gold, platinum and iridium isotopic chains [1]. For the even-Z mercury and platinum nuclei a sudden increase in the nuclear deformation appears at $A = 185$ and the odd-A nuclei also appear more deformed than even-even nuclei in the $A < 186$ region [2–4]. It has also been shown that the nuclear deformation of the odd-A platinum nuclei, with $A < 186$, depends upon the state occupied by the single neutron [4,5]. For the odd-Z nuclei, the nuclear deformation depends on the state occupied by the single proton resulting in different deformations in the thallium nuclei with $A < 194$, a sudden increase of the deformation for $A < 187$ in the gold and iridium nuclei and a shape coexistence in the ^{191,193}Tl and ^{186}Ir isotopes [6–11].

Nuclear shape coexistence has been found in nuclei close to the neutron-deficient lead nuclei from nuclear spectroscopy measurements performed using radioactive decay and in-beam experiments [12,13]. For example, decoupled rotational bands built on states arising from the $h_{9/2}$ sub-shell have moments of inertia indicating well-deformed nuclear states in the odd-A gold nuclei with

[a] e-mail: sauvage@ipno.in2p3.fr
[b] *Present address*: Universidad Complutense, Madrid, Spain.
[c] *Present address*: LBNL, Berkeley, CA, USA.
[d] *Present address*: Lawrence Livermore National Laboratory, Livermore, USA.
[e] *Present address*: Universidad de Sevilla, Sevilla, Spain.
[f] *Present address*: ANL, Argonne, IL, USA.
[g] *Present address*: VITO, IMS, Mol, Belgium.

$A < 190$. This band is built on a $9/2^-$ state located at 325 keV in ^{189}Au [14,15] and on the well-deformed $5/2^-$ ground state in ^{185}Au [16,17]. In the even-A mercury nuclei with $A < 190$, rotational bands are built on excited 0^+ states and correspond to a well-deformed nuclear shape. The energy of the 0^+ deformed state decreases when N lowers. However, the 0^+ deformed state remains an excited state and never becomes the ground state even at the neutron mid-shell $N = 104$ [18–21] whereas the well-deformed nuclear state $1/2^-[521]$ is the ground state of the odd-A ^{185}Hg nucleus. The properties observed in the lead nuclei appear to be similar to those known in the mercury nuclei: i) 0^+ states have been observed at low energy in ^{186,188}Pb nuclei [22], ii) quasi-rotational bands, built on $2_1{}^+$ states, have moments of inertia indicating the existence of a deformed nuclear shape for the excited states in the even-A $^{182-190}$Pb isotopes [23–26] and, iii) the energy of the $2_1{}^+$ state varies slowly against the mass, its value is the smallest ($E = 662$ keV) for $A = 186$ but remains higher than that of the $0_2{}^+$ and $0_3{}^+$ states. The ^{186,188}Pb results were recently confirmed in more complete studies [27,28]. Furthermore, the first excited band of ^{186,188}Pb has been determined to have a deformation of $\beta = 0.29$ by lifetime measurements [29]. The question remains whether a state corresponding to a well-deformed nucleus could become the isomeric or ground state in the odd-A lead isotopes close to the neutron mid-shell, in spite of their magic proton number $Z = 82$.

No shape transition or coexistence has been observed for the isomeric or ground states of the $^{190-214}$Pb nuclei from the isotope shift values measured using the atomic beam or collinear spectroscopy [30,31]. Recently, the deformation investigation was extended to the $^{182-190}$Pb nuclei using a highly sensitive in-source laser spectroscopy technique [32]. The hyperfine spectra are obtained by counting the radiation emitted by the nuclei of the photoionized atoms as a function of the laser frequency. The $^{182-188}$Pb nuclei have short half-lives ($T_{1/2} < 25$ s) and their α branching ratios ($b > 5\%$) are high enough to be used for the hyperfine spectrum recordings. On the other hand, the $^{189-190}$Pb nuclei have longer half-lives and small α branching ratios ($b < 1\%$), which made it necessary to use the γ-emission following β^+/EC decay to observe the hyperfine spectra. As a prerequisite, γ-ray identification has been performed since very little was known on the β^+/EC decay of ^{189}Pb [33]. In the course of this first experiment, qualitative hyperfine spectra and some γ-γ-t coincidence events were recorded for the γ-rays emitted from the ^{189}Pb decay. The results of this first experiment suggested that a low-spin isomer exists in ^{189}Pb, however, the observed coincidence relationships were incompatible with the level scheme of ^{189}Tl reported in ref. [34]. A second experiment has been performed in order to confirm the existence of a low-spin isomer in ^{189}Pb, to determine unambiguously the origin of the observed γ-rays, to establish a low-lying level scheme of the ^{189}Tl nucleus and to obtain more precise hyperfine spectra of the ^{189}Pb nucleus.

In this paper we present the results on the β^+/EC decay of ^{189}Pb (^{189}Pb $\rightarrow$ ^{189}Tl) obtained during the two experiments. The isotope shift and magnetic moment results [35] and the results on the α decay of ^{189}Pb (^{189}Pb $\rightarrow$ ^{185}Hg) will be reported elsewhere. After a description of the experimental procedures in sect. 2, the obtained data which allowed us to identify for the first time the radiation emitted either from the ^{189g}Pb or from the ^{189m}Pb isomer, as well as a level scheme of ^{189}Tl, will be presented and discussed in sect. 3. Finally, the low-lying levels of ^{189}Tl will be tentatively identified with the help of the semi-microscopic axial-rotor coupled to one quasi-proton model developed in the context of the Hartree-Fock plus BCS approximation [36].

2 Experimental procedures

Two experiments were carried out at the ISOLDE facility at CERN [37]. Radioactive lead atoms were produced via spallation reactions by bombarding a thick uranium-carbide, UC_x, target with the 1.4 GeV pulsed proton beam delivered by the PS-Booster. The radioactive atoms released from the target effuse into the hot cavity of the Resonance Ionization Laser Ion Source (RILIS) [38,39]. The lead atoms are then selectively ionized in a three-step resonant ionization process. The frequency scan is performed on the laser beam that produces after frequency doubling the first excitation step ($\lambda = 283.3$ nm). A laser beam of $\lambda = 600.2$ nm is used to get the second excitation step and the ionization step is provided by laser beams of $\lambda = 511$ and 578 nm (for more details, see refs. [32,35]). The thallium atoms are easily ionized, therefore, in spite of the selectivity of the RILIS method the lead ion beam is contaminated by the thallium atoms that are surface ionized in the hot cavity. The produced ions are extracted by 60 keV, mass-separated by the General Purpose Separator, GPS, guided towards the counting station, collected on a tape and then the obtained radioactive source is moved in front of the detectors.

In the first experiment the setup consisted of a 4π-β plastic scintillator detector and three γ detectors; one planar Ge(HP) X-ray detector with a 0.55 keV FWHM resolution at 80 keV and 0.9 keV at 356 keV, two coaxial Ge(HP) detectors with about 70% relative efficiency and 2.5 keV, 2.9 keV FWHM resolution at 1.33 MeV. The ISOLDE tape transport system was used to move the radioactive source from the collecting point to the counting setup.

To identify the γ-ray lines which belong to the ^{189}Pb decay (^{189}Pb $\rightarrow$ ^{189}Tl), singles γ spectra were recorded with the laser beam tuned on a resonant frequency expected for the low-spin isomer of ^{189}Pb and then on a resonant frequency expected for the high-spin isomer of ^{189}Pb. Singles γ spectra were also recorded without the laser beam to identify the γ lines due to the ^{189}Tl decay (^{189}Tl $\rightarrow$ ^{189}Hg) or due to background radiation. For these three measurements the ion beam was collected during a collecting time $t_c = 6$ s, starting 10 s after a proton pulse and the γ-rays from the sources were counted for a measuring time $t_m = 600$ s.

To observe hyperfine spectra two laser frequency scans were performed. In order to control the stability of the

experimental system, the laser frequency, ν, was tuned to a reference frequency after every third-frequency step. For every frequency step two sources were collected for $t_c = 2\,s$, starting 8 s after a proton pulse. The total measuring time for the two sources was $t_m = 223\,s$. The ISOLDE tape transport system was limited by the tape length and, therefore, only 21 frequency steps, 6 of them for the reference frequency, were taken at one time. The scanned frequency range was from $\nu = 17643.03$ up to $\nu = 17643.63\,cm^{-1}$ with a step $\delta\nu = 0.04\,cm^{-1}$. The reference frequency was $\nu = 17643.3299\,cm^{-1}$.

This combined nuclear and atomic spectroscopy method has been used for the first time to successfully study the α decay of the ^{185m,g}Pb isomers [40].

In the second experiment we used a more advanced tape transport system [41] with precise and reliable movements. Two counting stations were installed. The first station was placed at the collecting point to observe possible γ-rays emitted by nuclei decaying with short half-lives. It consisted of two γ detectors with Be windows, the planar Ge(HP) X-ray detector as described above, and one coaxial Ge(HP) detector with 18% relative efficiency and 1.9 keV FWHM resolution at 1.33 MeV. The second counting station, located at about 1 m above the collecting point, consisted of three detectors, one implanted Si α detector (100 mm^2 area and 100 μm thickness) with 14 keV FWHM resolution at 5.7 MeV and two coaxial Ge(HP) γ detectors one with 60% relative efficiency and 3.6 keV FWHM resolution at 1.33 MeV and the other with 70% relative efficiency and 4.3 keV FWHM resolution at 1.33 MeV. The rather poor resolution of these two detectors was partly due to electronic noise created by the laser system. In the first experiment it was shown that the counting rate was much weakened in the β-γ coincidence mode because the EC decay of the ^{189}Pb nucleus is not negligible, therefore, the 4π-β detector was not installed.

To identify the γ lines belonging to the ^{189}Pb decay, γ-γ coincidence measurements were performed for 10 hours at the 17643.20 cm^{-1} laser beam frequency for which both the ^{189m}Pb and ^{189g}Pb isomers are expected to be ionized with a good efficiency. The ion beam was collected for $t_c = 300\,ms$ immediately after the proton pulse and measured for $t_m = 52\,s$ after the tape movement ($t_d = 315\,ms$).

Subsequently, hyperfine spectra were recorded using the same procedure as before but with 38 frequency steps, 10 of them at the reference frequency. To obtain a more accurate frequency determination from the hyperfine spectra, the frequency step size was decreased to $\delta\nu = 0.02\,cm^{-1}$ and the reference frequency was $\nu = 17643.20\,cm^{-1}$. For every frequency step only one source was collected for $t_c = 2.5\,s$ immediately after the proton pulse and measured for $t_m = 54\,s$ after the tape movement. Four frequency scans have been executed: two using increasing frequency values and two with decreasing frequency values.

For the two experiments a data COMET-NARVAL acquisition system [42] has been used. The COMET card serves to determine the energies and time correlations (with a step $\delta t = 400\,ps$) of the detected radiations. For each detected radiation the energy and corresponding time are encoded and associated to create an event. Then, the NARVAL software sends all the events and the laser frequency to be recorded on disk and builds on-line control spectra. All information being preserved on disk coincidence events can be constructed off-line for any given coincidence window, and sorted to get γ-γ-t coincidence as well as γ-t and ν-γ matrices.

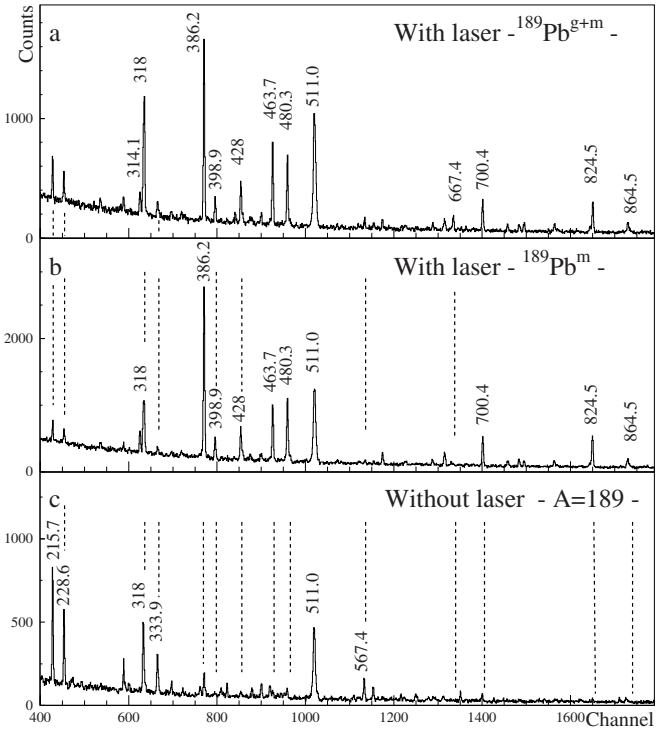

Fig. 1. γ spectra obtained with the laser beam tuned on the resonant frequency expected to ionize a) the low-spin and high-spin or b) only the high-spin ^{189}Pb isomer and c) the one obtained without the laser beam. The γ-line energies are given in keV.

3 Results

3.1 First experiment

Figure 1 shows the γ-ray spectra recorded with the laser beam tuned on the resonant frequency expected for the low-spin and high-spin ^{189}Pb isomers and without the laser beam. The 215.7, 228.6, 333.9 and 567.4 keV γ lines have a stronger intensity in fig. 1c, which indicates that they belong to the β^+/EC decay of the ^{189}Tl nuclei. The 314.1, 386.2, 398.9, 428, 463.7, 480.3, 700.4 and 824.5 keV γ lines have strong intensities in figs. 1 a and b. All these lines except the 824.5 keV γ line have also been observed in in-beam experiments [34,43,44], which strongly suggests that they belong to the β^+/EC decay of the ^{189}Pb high-spin isomer. In fig. 1a, one 667.4 keV γ line appears with a weak intensity and is not observed in figs. 1 b and c, therefore, it is a good candidate for the β^+/EC decay of

the ^{189}Pb low-spin isomer. The 318 and 463.7 keV γ lines are higher in fig. 1a than in fig. 1b, which suggests that they could be fed partly from the ^{189}Pb low-spin isomer. We have to note that the 318 keV γ line is observed in the three γ-ray spectra implying that it is, at least, a doublet. A 317.8 keV γ line belonging to the ^{189}Tl decay has been identified by Gowdy [45]. 317 keV and 319.7 keV γ lines were observed in a decay study of the ^{189}Pb nuclei [33] and the 319 keV γ line is believed to be the γ-ray transition linking a $3/2^+$ state to the $1/2^+$ ground state of the ^{189}Tl nucleus [13,33,46], which means that the 319 keV could belong to the decay of the ^{189}Pb low-spin isomer. Therefore, the high intensity of the 318 keV γ line observed in fig. 1a could be due to a strong feeding of the ^{189}Tl from the β^+/EC decay of the ^{189}Pb low-spin isomer and/or to the decay of the ^{189}Pb low-spin isomer.

The data recorded during the frequency scans were used to obtain X-ray and γ-ray singles spectra and γ-γ-t and ν-γ matrices. In spite of the low statistics of the γ-ray spectra taken with the planar detector, the 318 keV γ line is clearly observed as a doublet: a 317 keV and a 319 keV belonging to the decay of ^{189}Tl and ^{189}Pb nuclei, respectively. Further evidence is found in the γ-γ-t matrix, where the 319 keV γ line belonging to the ^{189}Pb decay is also clearly a doublet. The 463.7 and 428.3 keV γ lines are observed in coincident spectra for gates set on γ-rays at about 318 and 319 keV, respectively.

Although, precise hyperfine spectra were not achieved in the first experiment because of the technical limitations mentioned above, a few conclusions could be drawn. We obtained qualitative hyperfine spectra for the primary γ lines. The hyperfine spectra of the 667.4 keV γ line have a very poor statistics, however, they are similar to that of the low-spin isomer of the ^{185}Pb isotope. The hyperfine spectra of all the other γ lines are similar to the hyperfine spectrum of the high-spin isomer of the ^{185}Pb isotope [40].

The results of this first experiment suggest that a low-spin isomer exists in ^{189}Pb and that the 667.4 keV γ line belongs to its β^+/EC decay. The 318 keV γ line is a triple line in agreement with the results reported in refs. [33,45]. On the other hand, the 318, 463.7 and 428 keV γ lines have coincidence relationships that contradict the level scheme established from in-beam experiment results [34]. Furthermore, the hyperfine spectra of the 319 keV are not similar to that of the low-spin isomer of the ^{185}Pb isotope [40], which raises doubts on the identification of the 319 keV γ line given in refs. [13,33,46].

3.2 Second experiment

Since no γ-ray emitted by nuclei having half-lives shorter than 30 s was observed with the collection-point counting setup, only the results that have been obtained using the setup installed 1 m above the collection point (see sect. 2) are presented below.

The data recorded at the fixed frequency $\nu = 17643.20\,\mathrm{cm}^{-1}$ of the laser beam have been used to obtain singles γ spectra as well as γ-γ-t and γ-t matrices. Singles γ spectra were analysed using the GAMANAM curve-fitting code [47], a modified version of the GAMANAL code [48]. A ^{152}Eu radioactive source was used for energy and efficiency calibrations. The energies and intensities of the γ-rays belonging to the β^+/EC decay of the ^{189}Pb isomers are listed in table 1. Four γ-γ matrices have been built: two for prompt coincidence events with coincidence window times of $t_w = 160$ ns and 400 ns, and two for delayed coincidence events with $t_w = 120$ ns shifted by 80 ns with respect to the prompt window. These matrices have been treated using a graphic analysis software for one- and two-dimensional histograms [49]. Coincident spectra obtained for gates on important γ lines are displayed in figs. 2–5 and the coincidence relationships are given in table 1.

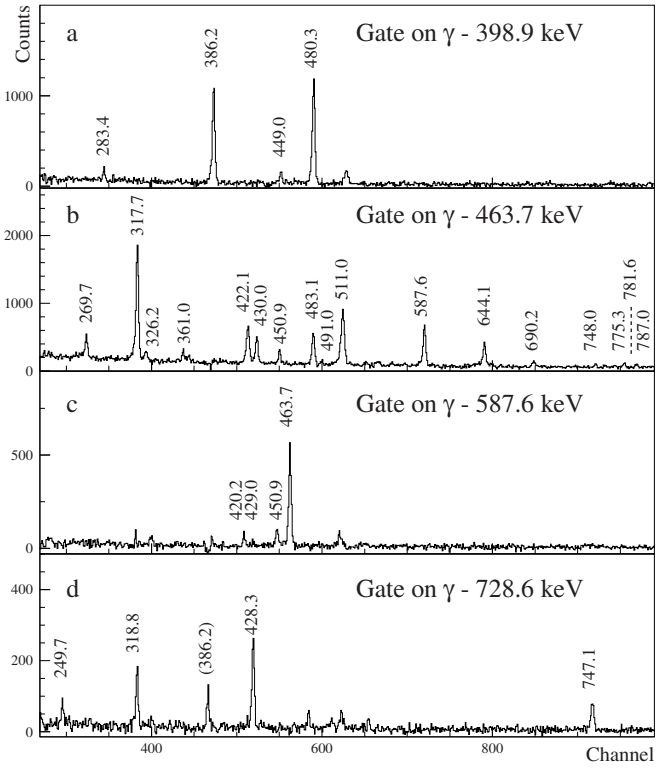

Fig. 2. Prompt coincident γ spectra for gates set on a) the 398.9, b) 463.7, c) 587.6 and d) 728.6 keV γ lines. The coincident γ line indicated in parentheses in d) is due to a contribution of the 730 keV γ line in the 728.6 keV gate. The γ-line energies are given in keV.

Four ν-γ matrices corresponding to the four frequency scans have been built. Gates have been set on the γ lines with intensity larger than 5% relative to the 386.2 keV γ line, the hyperfine spectra so extracted served to obtain information on the origin of the corresponding γ-rays. The results obtained from these four scans are very similar. The hyperfine spectra obtained for 386.2 keV gated γ lines have the structure expected for the 13/2 high-spin ^{189}Pb isomer, whereas the hyperfine spectra for gates set on the 667.4 keV γ lines are completely different and correspond to the structure expected for the 3/2 low-spin ^{189}Pb isomer. The hyperfine spectra obtained for gates set on the 825, 657; 464, 782; 865, 821; 588, 644; 422 and 318, 428 keV

Table 1. γ-ray data for the β^+/EC decay of the ^{189}Pb nucleus. γ-line intensities are given relatively to that of the 386.2 keV γ line ($I_\gamma = 100$). Parentheses mean uncertain coincidence relationship or tentative location.

$E_\gamma^{(a)}$ (keV)	$I_\gamma^{(b)}$	Main coincident γ-rays	Location
165[c]	~ 0.9		1227.6 → 1062.6
166.4	~ 2	314.1, 386.2, 398.9, 700.4, (613.6)	1147.5 → 981.4
194.0	~ 1.7	821.2	1614.8 → 1421.0
217.5	1.7	(667.4)	885.4 → 667.4
249.7	0.6	728.6, (318.8, 428.3, 747.1)	2006.4 → 1757.0
269.7	3.4	317.7, 420.2, 450.9, 463.7, 781.6	1332.3 → 1062.6
283.4[c]	~ 0.4	(824.5)	(1388.8 → 1105.3)
283.4	~ 0.9	386.2, 398.9, 480.3	1829.7 → 1546.4
292.6	0.9	318.8, 864.5	1757.0 → 1464.3
314.1	13	166.4, 386.2, 427.1, (398.9, 664.5, 896.0, 978.2)	981.4 → 667.2
317.7[d]	11	269.7, 463.7, (165.0, *562.7, 611.2*)	1062.6 → 744.7
318.8	20(10)[e]	428.3, 728.6, 821.2, 864.5, 934.1, 1015, (292.6, 784.6, 956.0)	599.8 → 281
318.8	29(10)[e]	1050.1, 1171, 1397.9	318.8 → 0
326.2	0.9	317.7, 463.7	1388.8 → 1062.6
336.3	1.0	(821.2)	1757.0 → 1421.0
348.5[d]	~ 0.8	318.8, 864.5	1812.6 → 1464.3
355.6	0.6	(824.5)	1460.9 → 1105.3
361	~ 1.7	427.5, 824.5	1893.8 → 1532.8
361[c]	~ 1.7	463.7	1105.3 → 744.7
365.1	2.3	667.4	1032.5 → 667.4
372.5	0.5	(318.8, 784.6)	2185.1 → 1812.6
386.2	100	314.1, 398.9, 427.1, 437.8, 480.3, 613.2, 657.2, 682.1, 741.5, 885.5, (283.4, 449.0, 536.4, 560.3, 664.5, 730, *751.5*, 978.2, 1094.4, *1138.0*, 1197.7, 1211.4, 1507.2)	667.2 → 281
391.4	2.5	318.8, *667.4*, 821.2	1812.6 → 1421.0
398.9	11	166.4, 283.4, 386.2, 449.0, 480.3	1546.4 → 1147.5
420.2	1.3	(269.7, 587.6)	1752.7 → 1332.3
422.1	5.0	463.7	885.4 → 463.7
427.1	~ 3.5	314.1, 386.2, 700.4	1408.6 → 981.4
427.5[c]	~ 7	361, 437.8, 824.5	1532.8 → 1105.3
428.1[c]	~ 3	(292.6, 428.3, 747.1)	2185.1 → 1757.0
428.3	~ 9	318.8, 728.6, 784.6, (934.1)	1028.1 → 599.8
429[c]	~ 1	587.6	(1761.2 → 1332.3)
430.0	5.4	317.7, 463.7, 781.6	1492.6 → 1062.6
437.8	2.6	386.2, (427.5)	1105.3 → 667.2
439.9[d]	~ 0.9		
449.0	~ 1.4	398.9, 480.3, (386.2)	1995.4 → 1546.4
450.9[d]	~ 1.7	(269.7, 463.7, 587.6)	1783.2 → 1332.3
463.7	33(3)[e]	269.7, 317.7, 430.0, 450.9, 483.1, 587.6, 644.1, *775.3*, (326.2, 361, 690.2, 787)	744.7 → 281
463.7	13(3)[e]	422.1	463.7 → 0
480.3	37	283.4, 386.2, 398.9, 449.0, 613.2, 682.1, (730, *785.3*, 1027)	1147.5 → 667.2
483.1	4.8	463.7	1227.6 → 744.7
491.0	0.6	(317.7, 463.7, 781.6)	1552.7 → 1062.6
498[c]	~ 0.4		(1962.2 → 1464.3)
536.4	2.0	657.3, 1044.3, (*318*, 386.2)	1861.3 → 1324.8
541.8	0.9	(318.8, *463.7*, 864.5)	2006.4 → 1464.3
560.3	2.0	(386.2), (*317, 333.9, 405.8*)[f]	(1227.6 → 667.2)
562.7	1.3	XTl+XHg, (*317.7*)	
587.6	7.2	420.2, 450.9, 463.7, (429)	1332.3 → 744.7
611.2[c]	~ 0.9	*317.7*	
613.2[d]	~ 1.7	386.2, 480.3, (700.4)	1761.2 → 1147.5
644.1	5.1	463.7	1388.8 → 744.7
657.2	10	386.2, 536.4	1324.8 → 667.2
664.5	1.9	314.1, 386.2, 700.4	1645.9 → 981.4

Table 1. Continued.

$E_\gamma^{(a)}$ (keV)	$I_\gamma^{(b)}$	Main coincident γ-rays	Location
667.4	9.6	217.5, 365.1, (*391.4, 439.9*)	667.4 → 0
682.1	1.4	386.2, 480.3, 700.4	1829.7 → 1147.5
690.2	1.2	463.7, 781.6, (317.7)	1752.7 → 1062.6
700.4	23	166.4, 427.1, 664.5, 896.0, 978.2, (398.9, 613.2)	981.4 → 281
720[c]	∼ 0.9	318.8, 864.5	2185.1 → 1464.3
728.6	5.4	249.7, 318.8, 428.3, 747.1	1757.0 → 1028.1
730[c]	∼ 0.9	(386.2, 480.3)	1877.8 → 1147.5
741.5	6.8	386.2	1408.6 → 667.2
747.1	8.0	728.6, 784.6, 934.1	1028.1 → 281
748[c]	∼ 0.7	(463.7)	1492.6 → 744.7
751.5	1.0	(*386.2*)	
775.3	0.6	(463.7)	
781.6	7.6	269.7, 326.2, 430.0, (450.9, 690.2)	1062.6 → 281
784.6[c]	∼ 1.7	318.8, 428.3, 747.1, (372.5)	1812.6 → 1028.1
785.3	∼ 1.7	XTl	
787[c]	∼ 0.7	(463.7)	(1532.8 → 744.7)
811.9	0.6		(1959.6 → 1147.5)
821.2	7.3	318.8, 336.3, (194.0, 391.4)	1421.0 → 599.8
824.5	30	355.6, 361, 427.5, (919.9, 1108.0)	1105.3 → 281
848.4	0.6	XTl	
860.0	1.8	(657.2, 1044.3)	2185.1 → 1324.8
863[c]	∼ 0.9	(314.1, 386.2, 700.4)	1844.4 → 981.4
864.5	13	292.6, 318.8, 348.5, 956.0, (372.5, 498.0, 541.8, 720)	1464.3 → 599.8
880.0	1.3	(314.1, 386.2, 700.4)	1861.3 → 981.4
885.5	2.3	386.2	1552.7 → 667.2
896.0	1.7	386.2, 700.4	1877.8 → 981.4
919.9	1.4	824.5	2025.2 → 1105.3
934.1	1.1	318.8, (428.3, 747.1)	1962.2 → 1028.1
947.2	1.7	XTl	
956.0	1.1	318.8, 864.5	2420.3 → 1464.3
978.2[c]	∼ 2.3	700.4, (314.1, 386.2)	1959.6 → 981.4
981.4	2.2	XTl	
1005.5	1.6	XTl	
1012.8	3.7	XTl	
1015[c]	∼ 1.7	(318.8)	1614.8 → 599.8
1027[c]	∼ 0.9	(386.2, 480.3)	2174.4 → 1147.5
1041.3	1.2	XTl	
1044.3	5.0	(536.4)	1324.8 → 281
1050.1	2.8	(318.8)	(1368.9 → 318.8)
1094.4	1.0	386.2	1761.2 → 667.2
1108.0	1.0	(824.5)	2213.3 → 1105.3
1117.2	1.6	XTl	
1138.0	4.1	(386.2)	
1171[c]	∼ 2.6	(318.8)	(1489.8 → 318.8)
1179.3	2.5	XTl	
1197.7	1.7	386.2	1864.9 → 667.2
1211.4	2.0	386.2	1877.8 → 667.2
1250.4	1.3	XTl	
1253.9	1.9	XTl	
1272.8	4.4	XTl	
1314.4	1.7	XTl	
1369.8	1.2	XTl, (*386.2, 480.3*)	
1397.9	1.0	(318.8)	(1716.7 → 318.8)
1491.9	0.7	XTl	

Table 1. Continued.

$E_\gamma^{(a)}$ (keV)	$I_\gamma^{(b)}$	Main coincident γ-rays	Location
1507.2	1.8	386.2	2174.4 → 667.2
1523.7	1.9	XTl	
1555.3	1.8	XTl	
1579.5	1.7	XTl	

(a) $\Delta E_\gamma \sim 0.2$ keV for transitions with $I_\gamma > 3$. $\Delta E_\gamma \sim 0.4$ keV for the other transitions.
(b) $\Delta I_\gamma \sim 15\%$.
(c) Transition from coincident events.
(d) Transition mixed with descendant ones.
(e) Intensity determined from the hyperfine spectrum.
(f) Transition belonging to the descendant.

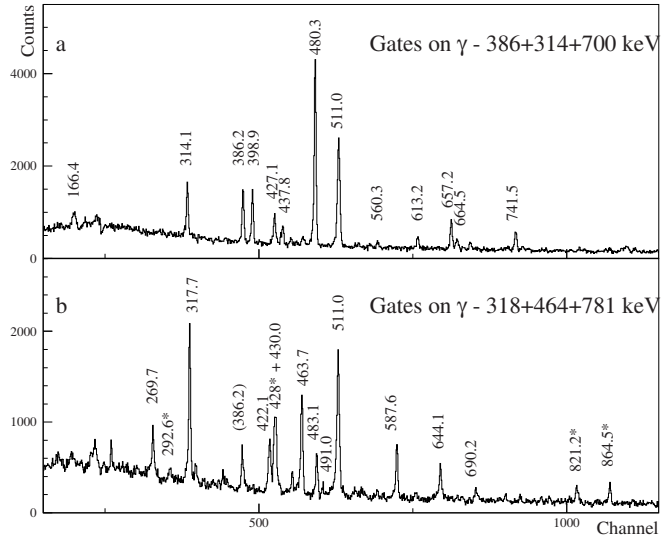

Fig. 3. Prompt coincident γ spectra for sum of gates set on a) the 386.2, 314.1 and 700.4 keV γ lines b) 318, 463.7 and 781.6 keV γ lines. In b) the coincident γ line given in parentheses is due to a contribution of the 314.1 keV in the 318 keV gate, asterisks indicate the coincident γ lines due to the 318 keV γ line of the part c) of the level scheme. The γ-line energies are given in keV.

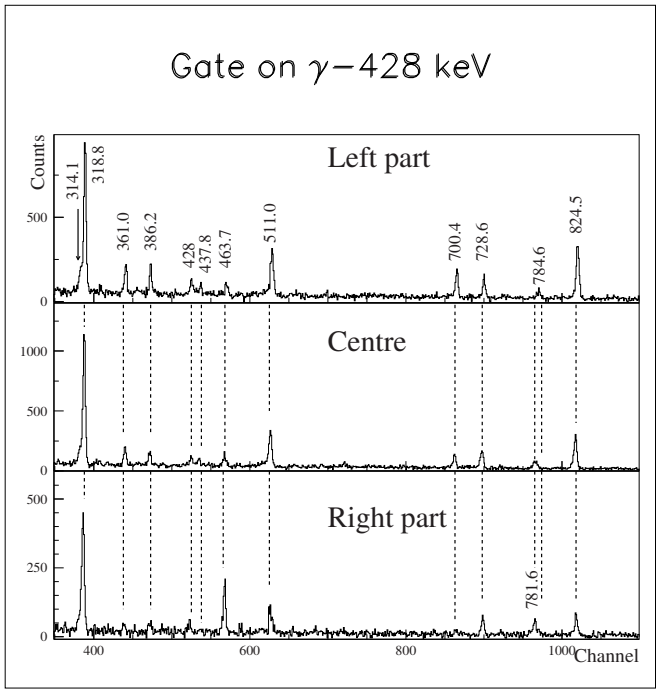

Fig. 4. Prompt coincident spectra for gates set on the left part, centre and right part of the 428 keV γ line. The γ-line energies are given in keV.

γ lines are shown with dotted lines in figs. 6 a, b, c, d, e and f, respectively, and are compared with the hyperfine spectra, drawn with solid lines, which have been extracted from the same frequency scan, for the 386 and 667 keV γ lines. We can see in fig. 6a that the hyperfine spectra for the 825 and 657 keV gates are very similar to that of the 386 keV gate, which unambiguously indicates that these two γ-rays are also emitted by levels fed from the high-spin ^{189}Pb isomer. The same conclusion can be deduced for the 782; 865, 821; 588, 644 and 428 keV γ-rays from figs. 6 b, c, d and f, respectively. On the other hand, the hyperfine spectrum for the 422 keV gate is similar to that of the 667 keV gate, indicating that the 422 keV γ-ray is from the low-spin ^{189}Pb isomer (see fig. 6e). The hyperfine spectrum extracted for the 318 keV γ line, shown (down triangles) in fig. 6f, has a small bump at a frequency value around $\nu = 17643.45\,\mathrm{cm}^{-1}$. This strongly suggests that part of the 318 keV γ-ray intensity could arise from the low-spin isomer. In the same way a very small bump is observed in the hyperfine spectrum obtained for the 464 keV gate, which could also correspond to a small feeding from the low-spin isomer (see fig. 6b, down triangles).

To determine the possible admixtures in the 464 and 318 keV γ lines, we have used the hyperfine spectra of the 386 and 667 keV γ lines to calculate hyperfine spectra corresponding to different admixtures. The calculated spectrum obtained if we assume that the high-spin and low-spin isomers feed the 464 keV γ line at 75% and 25%, respectively, has the best agreement with the experimental hyperfine spectrum with an estimated uncertainty of $\pm 5\%$. The experimental hyperfine spectrum of the 464 keV

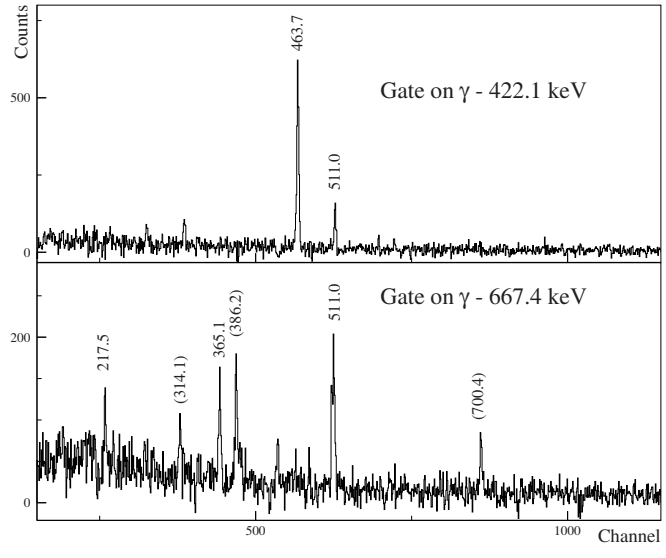

Fig. 5. Prompt coincident spectra for gates set on the 422.1 and 667.4 keV γ lines. Coincident γ lines given in parentheses are due to a contribution of the 664.5 keV γ line in the 667.4 keV gate. The γ-line energies are given in keV.

γ line, as a solid line, and the best calculated hyperfine spectrum, as circles linked with a dotted line, are shown in fig. 7. The case of the 318 keV γ line is more complicated since an important contribution is due to the decay of the ^{189}Tl nucleus. To simulate this contribution due to both the direct production of ^{189}Tl in the target and the decay of the ^{189}Pb isomers we have used the hyperfine spectrum of the 228 keV gate. None of the calculated hyperfine spectra reproduces exactly the experimental spectrum obtained for the 318 keV gate. The latter, shown with a solid line, is compared in fig. 7 to the hyperfine spectra calculated assuming the following contributions: i) 40% from the decay of ^{189}Tl, 35% from the low-spin ^{189}Pb isomer and 25% from the high-spin ^{189}Pb isomer (open circles) and ii) 40% from ^{189}Tl, 20% from low-spin ^{189}Pb isomer and 40% from the high-spin ^{189}Pb isomer (up triangles). The contribution due to the ^{189}Tl decay in the two calculated spectra is shown at the bottom. The structure of this contribution is due to the part of the ^{189}Tl coming from the ^{189}Pb decay, it can hence depend not only upon the percentage of the production by decay but also on the relative feeding from the low-spin and high-spin Pb isomers. The 228 and 317 keV γ lines belonging to the ^{189}Tl decay can have different feeding modes, which could explain why it is not possible to get a very good agreement between the experimental hyperfine spectrum of the 318 keV and the calculated spectrum whatever the admixtures assumed. Therefore, using a conservative estimate for the uncertainties, we obtain for the admixture in the 318 keV: 40 ± 10% from ^{189}Tl, 28 ± 10% from the low-spin ^{189}Pb isomer and 32 ± 10% from the high-spin ^{189}Pb isomer. Nevertheless, the intensities that are deduced from these results for the 464 and 318 keV, have been corrected for taking into account the different intensities observed in the γ singles spectra obtained during the coincidence measurement and the frequency scan and then, they have been reported in table 1. It is worth noting that the main intensity differences are observed for the γ-rays of the ^{189}Tl decay, the 228 keV γ-line relative intensity measured during the coincidence measurement is only 36% of that measured during the frequency scan.

3.2.1 Level scheme

The partial level scheme of ^{189}Tl was built from the γ-ray energies, intensities and coincidence relationships reported in table 1, as shown in fig. 8. The hyperfine spectra indicate very clearly that the three parts a, b and c, placed on the left-hand side of fig. 8, are fed by the $13/2^+$ high-spin ^{189}Pb isomer, which means that the lowest-energy states of every parts have spin values $I \geq 7/2$ (see below). Therefore, the a, b and c parts cannot be based on the $1/2^+$ ground state but on the $9/2^-$ isomeric state of the ^{189}Tl nucleus. Some weak links observed between the states of these different parts give support to their placement. Part d on the right-hand side of fig. 8 is fed from the low-spin ^{189}Pb isomer. No link could be found between the part d and the three other parts of the level scheme, therefore, we have located the first state of the parts a, b and c at 281 keV according to the energy suggested by Coenen *et al.* [46] from the energies of α-rays emitted by the ^{193}Bi isomers, the uncertainty of this energy is estimated to be ± 7 keV. It is worth noting that we show in this work that the 258 keV value proposed for the energy of the ^{189}Tl isomer in ref. [34] is wrong since the level scheme built in ref. [34] has to be modified (see also below the description of part b).

Part a of the level scheme consists of 23 levels, the 667.2, 981.4, 1147.5, 1408.6, 1546.4 1829.7 and 1995.4 keV levels correspond to states already observed in in-beam experiments [34,43,50], examples of coincident spectra for gates set on the 398.9 keV γ line and the sum of the gates set on the 386, 314 and 700 keV γ lines are displayed in figs. 2a and 3a, respectively. The 1645.9 keV level is due to the 664.5 keV γ line observed in coincidence with the 314.1, 386.2 and 700.4 keV γ lines (see table 1 and fig. 3a). This confirms the 664.5 keV γ-ray position in the level scheme given in refs. [34,43,44]. The 863.0 keV that de-excites the 1844.4 keV level confirms the results reported in refs. [34,44]. The 657.2 keV in coincidence with the 386.2 keV γ line, de-excites the 1324.8 keV level. This transition was only observed by Porquet *et al.* [43]. The 1861.3 keV level decays to both the 1324.8 and 981.4 keV states, which allowed us to confirm the position of the 657.2 keV γ line on the 667.2 keV state. An intense γ line has been observed at 824.5 keV; this line was never mentioned in in-beam works but was seen in a decay work [33]. However, its hyperfine spectrum clearly indicates that it belongs to the high-spin isomer decay (see fig. 6a). Moreover, it appears with the 437.8 keV γ line in the coincidence spectra obtained for gates set on the left part and at the centre of the 428 keV γ line, as can be seen in fig. 4. Therefore, the 824.5 keV γ-ray was put directly

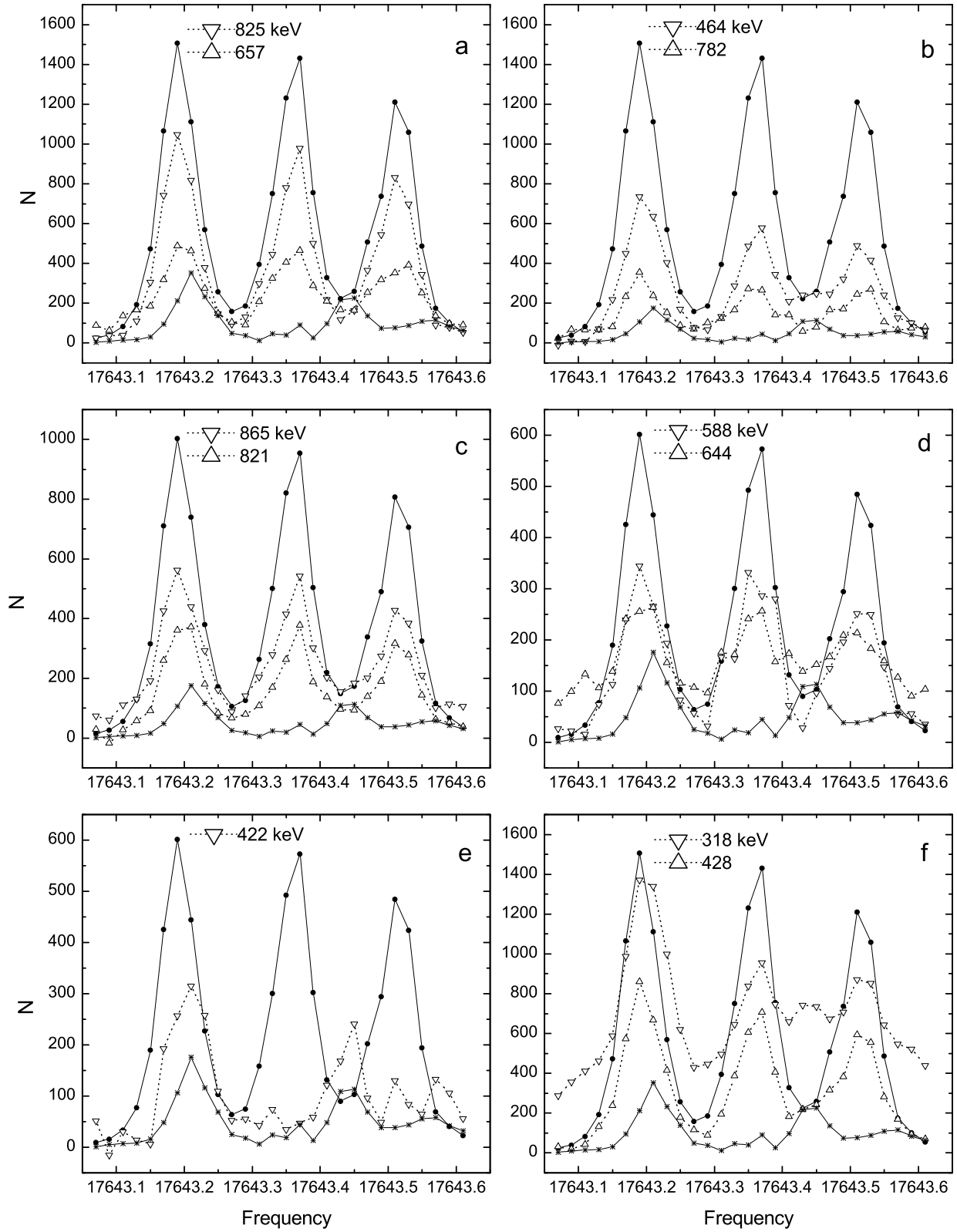

Fig. 6. Comparison of the hyperfine spectra obtained for gates set on the main γ lines (open triangles) with those for gates on the 386.2 (full circles linked with solid lines) and 667.4 keV (asterisks linked with solid lines) γ lines that correspond to the high-spin and low-spin ^{189}Pb isomers, respectively. All the hyperfine spectra have been obtained for gates set on the same ν-γ matrix but the intensities of those of the 386.2 and 667.4 keV gates have been divided by different factors to make the figures clearer (386.2 keV: $N/4$ in a), b) and f), $N/6$ in c) and $N/10$ in d) and e); 667.4 keV: $N/2$ in b), c), d) and e)). Frequency values in cm^{-1} correspond to the laser beam of the first excitation step before doubling.

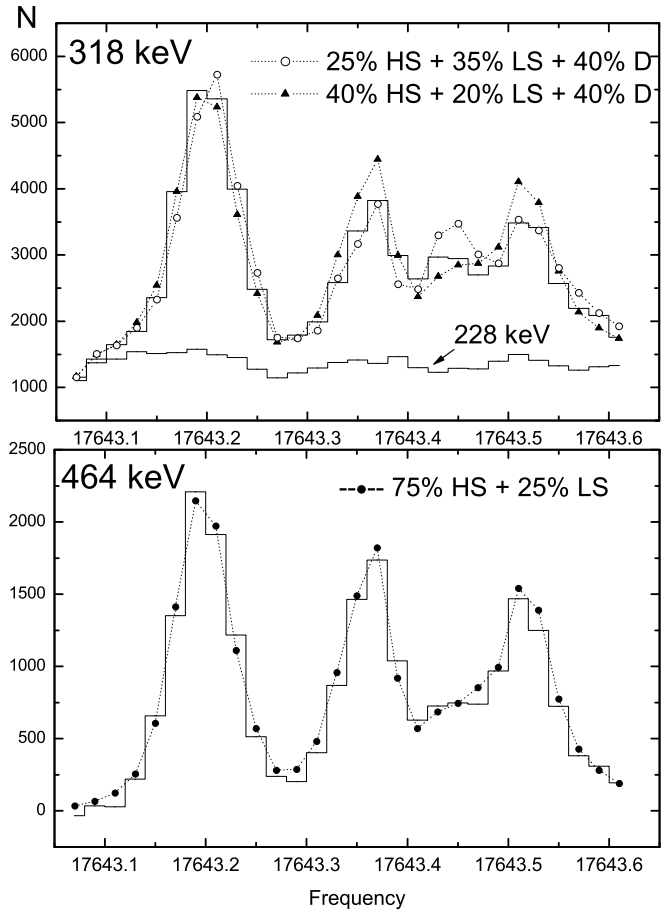

Fig. 7. Comparison of the hyperfine spectra observed for the 464 and 318 keV gates (solid lines) with the hyperfine spectra calculated assuming that the high-spin (HS) and low-spin (LS) isomers feed: i) the 464 keV γ line with 75% and 25%, respectively (full circles) and ii) the 318 keV γ line with 25% and 35% (open circles) or with 40% and 20% (full triangles), respectively, with in both cases a contribution of 40% of the ^{189}Tl decay (D). The hyperfine spectrum of the 228 keV gate that has served to simulate the contribution of the ^{189}Tl decay in the 318 keV γ line is shown at the bottom of the figure. Frequency values in cm^{-1} correspond to the laser beam of the first excitation step before doubling.

on the 281 keV level. Thus, an 1105.3 keV level was established as well as the 1460.9, 1532.8, 1893.8, 2025.2 and 2213.3 keV levels since they decay towards the 1105.3 keV state. Six other levels have been built from the coincidences observed with the 386, 480 and/or 700 keV γ lines.

Part *b* of the level scheme includes the 463.7, 317.7, 781.6, 269.7, 587.6, 430.0 and 450.9 keV γ lines that were also observed by Riedinger *et al.* [34] but we established a completely different level scheme from our coincidence relationships. From the level scheme of ref. [34] the 781.6, 450.9, 291 and 395 keV γ lines should be the main γ lines observed in coincidence with the 463.7 keV γ-ray. One can see in the coincidence spectrum of the 463.7 keV gate, shown in fig. 2b, that the 317.7 keV is much higher than the 450.9 keV γ line and that neither the 781.6 keV nor the 291 and 395 keV γ lines are observed. In the same way the 450.9 keV should be the main γ line observed in coincidence with the 587.6 keV γ-ray. In the coincidence spectrum of the 587.6 keV gate the 450.9 keV is very small compared to the 463.7 keV γ line (see fig. 2c). Thus, our results are in contradiction with the level scheme of ref. [34] and consequently indicate that the 258 keV value proposed for the energy of the ^{189}Tl high-spin isomer is wrong.

The hyperfine spectra shown in figs. 6 b and d indicate that the levels de-excited by the 587.6, 644.1 and 781.6 keV γ-rays are only fed by the high-spin ^{189}Pb isomer whereas the level de-excited by the 463.7 keV γ-ray should be fed at $25 \pm 5\%$ by the low-spin isomer. In addition to this, the 422.1 keV γ line which must de-excite a level only fed by the low-spin isomer (see fig. 6e), is in coincidence with the 463.7 keV γ-ray. The sum of the energies of these two coincident γ-rays is equal to 885.8 keV, this energy sum is very close to the energy of the cascade 217.5-667.4 equal to 884.9 keV. These facts strongly suggest that the 463.7 keV could be a doublet. For these reasons, the 422.1-463.7 keV cascade has been placed in part *d* of the level scheme. The relative intensity of this 463.7 keV transition is 13 ± 3 from the hyperfine spectrum (see table 1).

The 361 keV is in coincidence with both the 427.5 and 463.7 keV γ lines, and is about twice higher in the coincidence spectrum of the 427.5 keV gate than in that of the 463.7 keV gate (see figs. 2b and 4a). This means that the 361 keV is very likely a double line: one placed above the 427.5 keV transition and the other one under it. This latter is one of the links found between parts *a* and *b* of the level scheme. The other γ-rays that are possible links could not be confirmed since no γ transition was observed above the levels that these links de-excite. These links are seen as very weak peaks in the coincidence spectra: the 560.3 keV is in coincidence with the 386.2 keV γ line (see table 1 and fig. 3a), the 787 keV with the 463.7 keV γ line (fig. 2b), the 429 keV with the 587.6 keV γ line (fig. 2c) and the 491.0 keV with the 463.7 and 781.6 keV γ lines (see table 1, figs. 2b and 3b).

As for part *c* of the level scheme, the hyperfine spectra indicate that the levels de-excited by the 428.3 and 747.1, 821.2, 864.5 and 728.6 keV γ lines are fed by the high-spin ^{189}Pb isomer. On the other hand, the hyperfine spectrum of the 318.8 keV gate reveals that the contributions of the low-spin and high-spin isomer decays are about the same (see fig. 7). The 599.8 keV level that is linked by the 428.3 keV γ-ray to the 1028.1 keV level directly fed by the 13/2 high-spin isomer decay, is probably not fed directly by the low-spin isomer decay since its spin value is at least 7/2. This led us to conclude that the 318.8 keV γ line is a doublet. For these reasons, part of the 318.8 keV γ line has been attributed to part *d* of the level scheme. The relative intensity of this 318.8 keV γ line has been estimated at 29 ± 10 from the hyperfine spectrum.

The 657.2 and 1044.3 keV γ lines, de-exciting the level at 1324.8 keV, displayed in part *a* of the level scheme, have been observed in coincidence with the 860.0 keV γ line. This gives a level located at 2184.8 keV, an energy very close to the energy of a level established at 2185.1 keV in the part *c* of the level scheme. Thus, the 860.0 keV γ-ray is

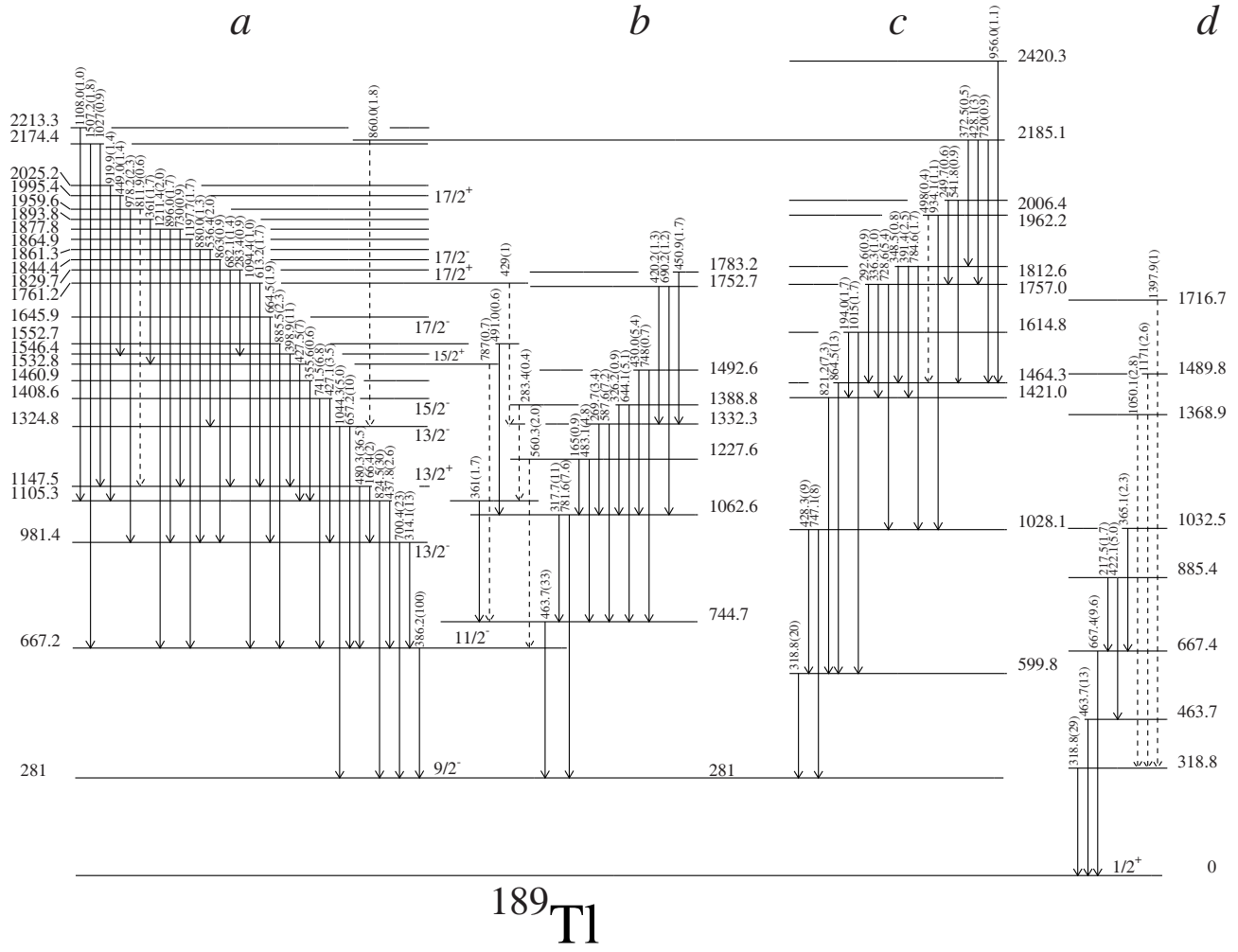

Fig. 8. Partial level scheme of the ^{189}Tl nucleus obtained from the β^+/EC decay of the ^{189}Pb isomers. The energy of the $9/2^-$ isomer is 281 ± 7 keV taken from ref. [46] (see text). The reported spin and parity values have been taken from refs. [34,43]. The part *d* of the level scheme, fed by the low-spin ^{189}Pb isomer, is tentative.

the only possible link we found between part *a* and part *c* of the level scheme.

Part *d* of the level scheme is built around the 667.4-217.5 keV cascade indisputably fed from the low-spin isomer of the ^{189}Pb nucleus. One can see in fig. 5 that the 667.4 keV is only in coincidence with the 217.5 and 365.1 keV γ lines. The parts of the 318.8 and 463.7 keV double γ lines that de-excite the levels fed from the low-spin isomer have been placed on the ground state. Unfortunately, their position could not be confirmed from other coincidence relationships since no γ-ray is observed above the 318.8 and 885.4 keV levels, therefore, their placement in the level scheme should be considered tentative.

Most of the γ lines identified as belonging to the β^+/EC decay of the ^{189}Pb isomers have been placed in the level scheme shown in fig. 8, which corresponds to 93% of the observed γ intensity. Given that i) no line with energy lower than 165 keV has been observed, ii) no level has lifetime long enough to observe delayed transitions in the matrices of delayed coincidence events, which eliminates the high multipolarities ($> M2$ and $M2$ for transition energy < 500 keV) for the observed transitions and iii) most of the transitions have an unknown multipolarity, a first qualitative level intensity balance has been performed using the γ line intensities. In table 2 the γ intensity balances have been listed for the levels that are fed at more than 5% of the 386.2 keV γ intensity or those that have a spin value attributed from in-beam works [34,43]. One can see that the γ balance value is positive for all levels except for the 599.8 keV one. If we assume an M1 multipolarity for the 318.8 keV transition that de-excites the 599.8 keV level, its total intensity is then equal to 26.6 whereas the total level feeding is equal to 31.8 ± 1.1, the error is estimated from the $E1$, $E2$ or $M1$ possible multipolarity of the four transitions that feed the level. This indicates an underestimation of this 318.8 keV transition intensity, the γ intensity should be at least 24 instead of 20 which is in agreement with the estimated error bar of the 318.8 keV line intensity (20 ± 10) reported in table 1. One can see from table 2 that the states with spin value 11/2, 13/2 or 15/2 are obviously the most fed levels from the β^+/EC decay of the $13/2^+$ isomer. It is clear that, in

Table 2. Intensity balances, log ft values, and spin and parity values for the most fed levels of the parts a, b and c of the level scheme, the 599.8 level and those that have spin and parity values assigned from in-beam experiments [34,43].

			Intensity balance for high-spin states							
$E_{\rm level}$	I^π		Feeding	Decaying	Balance		Feeding	$\log f_0 t$	$\log f_1 t$	I^π
keV	refs. [34,42]		I_γ	I_γ	I_γ	$I_{\rm tot}$	$I_{\rm tot}(\%)$			
599.8			31	20	−11		–			
667.2	$11/2^-$		80.2	100	19.8	$19.1 \ll 37.6$	11.0 ± 3.6	$6.04 \ll 6.34$	$8.0 \ll 8.3$	
981.4	$13/2^-$		14.2	36	21.8	$22.6 \ll 26.2$	9.5 ± 0.7	6.1	8.0	
1028.1			8.2	17	8.8	$10.0 \ll 10.5$	4.0 ± 0.1	6.5	8.4	$11/2^\pm$,$13/2^\pm$,$15/2^\pm$
1062.6			12.4	18.6	6.2	$2.3 \ll 9.8$	2.3 ± 1.5	$6.5 \ll 7.1$	$8.4 \ll 9.0$	
1105.3			10.4	34.3	23.9	$22.9 \ll 25.4$	9.4 ± 0.5	6.1	8.0	$11/2^\pm$,$13/2^\pm$,$15/2^\pm$
1147.5	$13/2^+$		16.5	39	22.5	$21.0 \ll 22.5$	8.4 ± 0.3	6.1	8.0	
1227.6				7.7	7.7	$7.8 \ll 10.2$	3.5 ± 0.5	6.5	8.4	$11/2^\pm$,$13/2^\pm$,$15/2^\pm$
1324.8		$13/2^-$	3.8	15	11.2	$11.2 \ll 11.7$	4.4 ± 0.1	6.4	8.2	
1332.3			4	10.6	6.6	$6.3 \ll 8.9$	2.9 ± 0.5	6.5	8.4	$11/2^\pm$,$13/2^\pm$,$15/2^\pm$
1388.8				6.4	6.4	$6.4 \ll 7.2$	2.6 ± 0.2	6.6	8.4	$11/2^\pm$,$13/2^\pm$,$15/2^\pm$
1408.6	$15/2^-$			10.3	10.3	$10.5 \ll 10.9$	4.1 ± 0.1	6.3	8.2	
1464.3			5	13	8	$7.3 \ll 8.3$	3.0 ± 0.2	6.5	8.4	$11/2^\pm$,$13/2^\pm$,$15/2^\pm$
1492.6				6.1	6.1	$6.2 \ll 6.9$	2.5 ± 0.2	6.5	8.4	$11/2^\pm$,$13/2^\pm$,$15/2^\pm$
1532.8			1.7	7.7	6	$7.8 \ll 8.8$	3.2 ± 0.2	6.4	8.3	$11/2^\pm$,$13/2^\pm$,$15/2^\pm$
1546.4	$15/2^+$		2.3	10.4	8.1	$8.7 \ll 10.4$	3.7 ± 0.3	6.4	8.2	
1645.9	$17/2^-$			1.9	1.9	1.9	0.74	7.0	8.9	
1829.7	$17/2^+$			2.3	2.3	$2.4 \ll 2.7$	0.99 ± 0.06	6.8	8.7	
1844.4		$17/2^-$		0.9	0.9	0.9	0.35	7.3	9.1	
1995.4	$17/2^+$			1.4	1.4	1.6	0.62	7.0	8.8	
2185.1				6.2	6.2	$6.2 \ll 6.8$	2.5 ± 0.1	6.3	8.1	$11/2^\pm$,$13/2^\pm$,$15/2^\pm$

this decay work, we can observe the states with spin value $\leq 17/2$ only. The 281 keV $9/2^-$ level cannot be directly fed from the $13/2^+$ isomer, therefore, it is possible to estimate the number of disintegrations of the high-spin ^{189}Pb isomer by summing up the intensities of the 8 transitions feeding the 281 keV level. Doing so we obtain 247 ± 12, where the error is due to the unknown transition multipolarities assumed to be only $E2$ or $M1$ since a positive parity is not probable for the low-lying levels under consideration (see further).

To determine the feedings to the states fed from the ^{189}Pb high-spin isomer we have used the transition multipolarities and spin values known from in-beam experiments [34,43] and assumed an $E2$ or $M1$ mutipolarity for the 317.7, 318.8, 428.3, 437.8, 463.7, 747.1, 781.6, 824.5 keV transitions and an $E1$, $E2$ or $M1$ multipolarity for the other transitions. We used the internal conversion coefficients of ref. [51]. The sum of the calculated feedings is equal to 258 ± 30, the error bar corresponds to only the unknown transition multipolarities. It is in good agreement with the number of disintegrations given above. The $\log f_0 t$ and $\log f_1 t$ values, for the most fed states ($\geq 2.3\%$) and for those with assigned spin and parity values, have been calculated using the $\log ft$ tables [52] with the obtained feedings, $Q_{\rm EC} = 6.76$ MeV [53,54] and $T_{1/2} = 51$ s (ref. [53]) and are reported in table 2. In spite of the missing multipolarities, the β^+/EC level feedings larger than 2.4% have rather small relative uncertainties ($< 17\%$) except for the 667.2 keV level feeding (33%). The calculated $\log f_0 t$ and $\log f_1 t$ values are smaller than 8.5 except for the 1062.6 keV and 17/2 levels, which means, from the Raman-Gove rules [55], that the β decay to these levels corresponds to allowed or first-forbidden non-unique transitions. Therefore, the spin value of these states is $I = 11/2$, $13/2$ or $15/2$ with a positive or negative parity (see the last column of table 2).

3.2.2 Half-lives

The measuring time $t_{\rm m} = 52$ s was too short to provide accurate decay half-life determination of the ^{189}Pb isomers. However, estimations were extracted from the γ-t matrix built from the singles γ data recorded during the γ-γ coincidence measurement. The time spectra obtained for gates set on the 386, 480, 667, 700 and 865 keV γ-rays were analysed by the conventional least-square method, χ^2 method, and the results were confirmed by fits performed using the Awaya method [56]. Then, the half-lives were corrected for the dead time of the acquisition system that is measured for every acquisition channel, the dead time due to pile-up in the amplifier is not taken into account: correction of $6.2 \pm 1.0\%$ for the half-life of the high-spin isomer from the 386.2 keV γ-ray and $5 \pm 0.8\%$ for that of the low-spin isomer from the 667.4 keV γ-ray. The results are the following: $T_{1/2} = 49.7 \pm 0.1$, 46.9 ± 0.2, 54.8 ± 0.5 s from the 386, 480 and 865 keV γ-rays, the given error bars are only due to statistical uncertainties. The Compton background represents only 24% of the total intensity for the 386 keV gate, whereas it is 63% for the 865 keV gate resulting in different uncertainties, which explains the different $T_{1/2}$ values. From these results, the half-life of the $13/2^+$

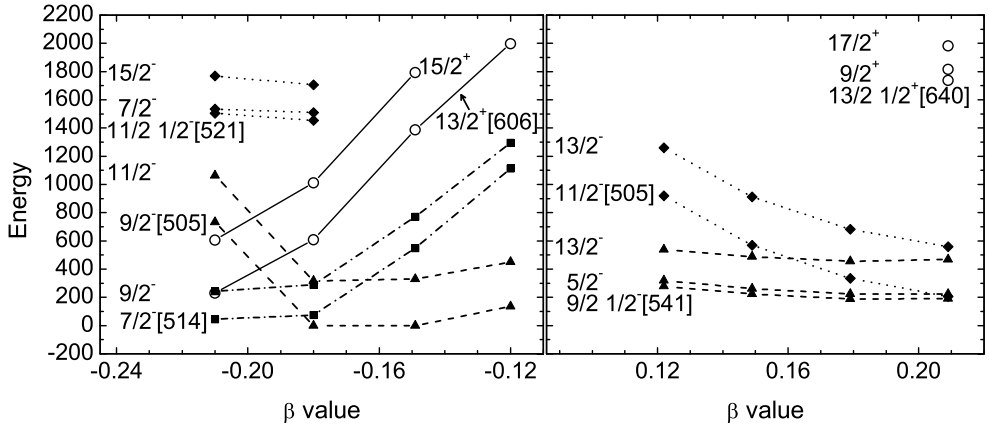

Fig. 9. Energy evolution of the first two members of every high-spin coupled states ($I > 5/2$) as a function of the deformation parameter β ($\beta < 0$ for oblate deformation, $\beta > 0$ for prolate deformation).

isomer of ^{189}Pb was estimated to be $T_{1/2} = 50 \pm 3$ s, in agreement with the value $T_{1/2} = 51 \pm 3$ s reported in the literature for ^{189}Pb [53]. Therefore, our result shows that this $T_{1/2}$ value has to be attributed to the $13/2^+$ isomer and not to the low-spin isomer of ^{189}Pb. The longer value $T_{1/2} = 63$ s found for the 700 keV gate could be due to the presence of a weak-intensity line with an energy close to 700 keV and belonging to a ^{189}Pb descendant or to the background noise. The half-life of the $3/2^-$ isomer of ^{189}Pb has been estimated to be $T_{1/2} = 39 \pm 8$ s from the 667 keV gate, the error bar is mainly due to the uncertainty on the Compton background subtraction that represents 71% of the total intensity for the 667 keV gate.

4 Discussion

To identify the low-lying levels established in ^{189}Tl we have used the semi-microscopic axial-rotor coupled to one-quasiparticle model described in ref. [36]. The quasiparticle wave functions, in the ^{188,190}Pb neighboring cores, have been obtained from HF plus BCS calculations [57–59] using the Skyrme III force [60] and the usual pairing interaction with constant matrix elements ($G_{0n} = 14.6$ and $G_{0p} = 13.3$ for Pb) and standard cut-off. The moments of inertia used in the calculations with the ^{188}Pb and ^{190}Pb cores have been deduced from the energies of the states built on the first 2^+ levels of the ^{188}Pb and ^{190}Pb nuclei located at 724 and 774 keV, respectively; the energies of the 0^+ states of these bands have been estimated by extrapolation of the variable moments of inertia of the excited bands.

Deformation parameters, β, for the $9/2^-$ isomer of the ^{189}Tl nucleus, have been deduced from laser spectroscopy measurements: $\langle\beta^2\rangle^{1/2} = 0.181$ from the isotope shift value assuming $\beta = 0$ for ^{207}Tl and $\beta = -0.153$ from the intrinsic quadrupole moment, Q_0, deduced from the measured spectroscopic quadrupole moment, Q_s, assuming strong coupling model and $K = I = 9/2$ (ref. [7]). The existence of a small component (few %) $K = 7/2$ in the wave function of the $9/2$ state would be enough to explain the smaller β value deduced from Q_s. In this mass region, it is well known that the nuclear deformation can depend on the state occupied by the coupled proton [6–11]. Thus, in ^{191}Tl, the β value obtained for the $9/2^-$ isomer is $\langle\beta^2\rangle^{1/2} = 0.16$ from the isotope shift value ($\beta = -0.142$ from the Q_s value) whereas for the $1/2^+$ ground state $\langle\beta^2\rangle^{1/2} = 0.112$ from the isotope shift value [8]. This led to calculate every coupled states for different deformations by constraining the quadrupole moment of the core in the HF plus BCS treatment. The energies and wave functions of the quasiparticle states in the ^{188,190}Pb cores have been determined for the following deformation parameters: $\beta = -0.21, -0.18, -0.15, -0.12, +0.12, +0.15, +0.18, +0.21$. It is worth noting that the results obtained using the two cores, ^{188,190}Pb, are similar. The energy evolution of the two first states of every coupled states as a function of the β value, obtained using the ^{190}Pb quasiparticle wave functions, is shown in fig. 9 for high-spin states ($I > 5/2$) and in fig. 10 for low-spin states ($I < 7/2$). In these figures the particle states are labelled with the quantum numbers, $I\,K[Nn_z\Lambda]$, of the main component of their wave function (I is the angular momentum of the state, K is the projection of I on the symmetry axis of the nucleus and N, n_z, Λ are the Nilsson asymptotic quantum numbers). We can note that for the rotational bands built on the $1/2^-[521]$ state corresponding to an oblate nuclear shape and on the $1/2^-[541]$ and $1/2^+[640]$ states corresponding to a prolate nuclear shape, the bandheads have $I = 11/2$, $I = 9/2$ and $I = 13/2^+$, respectively indicating a decoupling of the single-particle and core movements due to the Coriolis force.

4.1 High-spin states

The $\Delta I = 1$ structure of the rotational band built on the $9/2^-$ isomeric state is well reproduced with calculations performed assuming an oblate nuclear shape (negative β values). Moreover, the $9/2^-[505]$ state is predicted to be the first high-spin level for oblate shape with $\beta \geq -0.18$ (see fig. 9), which is in agreement with the deformation determined from the laser spectroscopy studies [7,8]. As seen in fig. 9 several other coupled states are expected to be lying at low energy in ^{189}Tl, $7/2^-[514]$ and $13/2^+[606]$

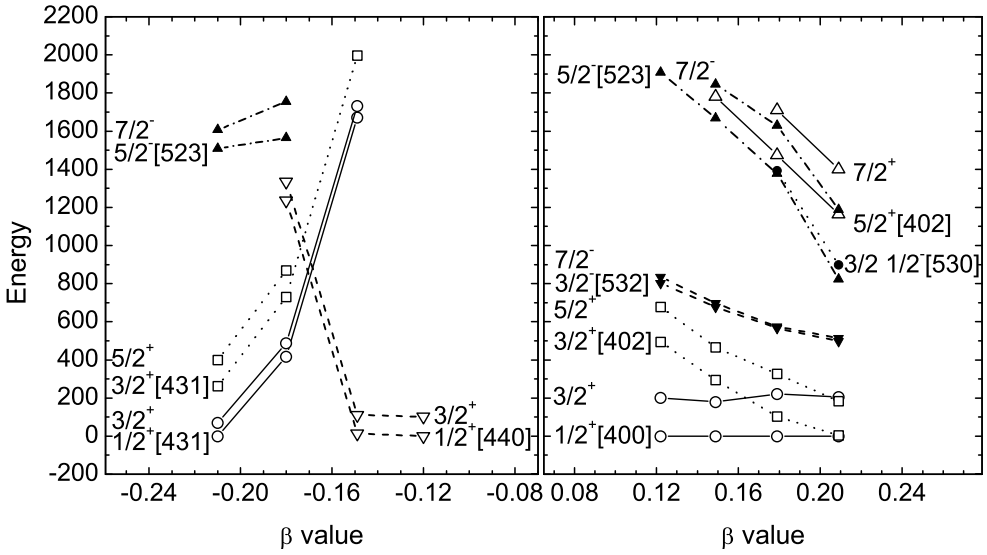

Fig. 10. Energy evolution of the first two members of every low-spin coupled states ($I < 7/2$) as a function of the deformation parameter β ($\beta < 0$ for oblate deformation, $\beta > 0$ for prolate deformation).

states with oblate nuclear shape and $9/2\ 1/2^-[541]$ (arising from the $h_{9/2}$ sub-shell) and $11/2^-[505]$ states with prolate nuclear shape.

The 1147.5, 1546.4 and 1829.7 keV levels observed in this work had already been identified as the $13/2^+$, $15/2^+$ and $17/2^+$ members of the $13/2^+[606]$ band from previous in-beam works [43,50]. Shown in fig. 9 the energy location of these states is well reproduced for an oblate deformation with $\beta \sim -0.17$.

The $7/2^-[514]$ state is predicted to be located above the $9/2^-[505]$ state and below the $13/2^+[606]$ state for an oblate deformation with $\beta \geq -0.18$ and it could be the established level at 744.7 keV. Furthermore, the 317.7-269.7-450.9 γ cascade observed in the present work and in in-beam work [34] could link the first members of the $7/2^-[514]$ rotational band, which leads us to assign the spin and parity values $I^\pi = 9/2^-$, $11/2^-$ and $13/2^-$ to the 1062.6, 1332.3 and 1783.2 keV levels, respectively. The weak feeding of the 744.7 and 1062.6 keV levels and the possible I^π values of the 1332.3 keV level deduced from the $\log ft$ values are in favour of these assignments.

The 1105.3 keV level, with $I^\pi = 11/2^\pm$, $13/2^\pm$ or $15/2^\pm$, decays to the $9/2^-$ level at 281 keV and the $11/2^-$ level at 667.2 keV. It decays also towards the 744.7 keV level proposed above as the $7/2^-[514]$ state. It is likely an $11/2^-$ level, therefore, it could be the $11/2^-[505]$ state predicted in the calculations performed assuming prolate deformations (see fig. 9). The 824.5 keV γ line that deexcites the 1105.3 keV level, has never been observed in in-beam experiments, which lends support to this last proposal. The $13/2^-$ member of the $11/2^-[505]$ band should be the 1460.9 keV rather than the 1532.8 keV level because of the possible link of the 1532.8 keV level with the $(7/2^-)$ 744.7 keV state.

The $9/2\ 1/2^-[541]$ state with a prolate nuclear shape is predicted to be located at a smaller energy than the $11/2^-[505]$ state for $\beta < 0.21$ and the rotational band built on it has a $\Delta I = 2$ decoupled structure. The 599.8 keV level could be assigned the $9/2\ 1/2^-[541]$ state; the 1028.1 level decays towards the 599.8 keV level and to the $9/2^-$ level at 281 keV would then be the $13/2^-$ state of the decoupled band. This hypothesis is in agreement with the fact that the 599.8 keV level is not directly fed by the Pb β^+/EC decay and with the possible I^π values of the 1028.1 level (see table 2). Anyway, the 599.8 keV level cannot be the $7/2^-[514]$ state because this hypothesis would lead us to attribute $I^\pi = 9/2^-$ to the 1028.1 keV level, which would be in contradiction with its possible I^π values. Furthermore, the $K = 1/2$ property of the 599.8 and 1028.1 keV levels can explain the absence of an observed link between these levels and the parts a and b of the level scheme. These linking transitions are indeed hindered due to their $\Delta K \geq 3$ character. The first level which could be the $17/2^-$ member of the decoupled band is the one located at 1757.0 keV.

To illustrate the quality of the agreement between experimental and theoretical results in the frame of the proposed state identification, the experimental levels identified above are compared with the theoretical states predicted from the ^{190}Pb core in fig. 11 for oblate and prolate nuclear states. We can see that the agreement is qualitatively good for the oblate $9/2^-[505]$, $7/2^-[514]$, $13/2^+[606]$ and prolate $11/2^-[505]$ states.

4.2 Low-spin states

From isotope shift measurements the deformation parameters of the $1/2^+$ ground states of ^{193}Tl and ^{191}Tl have been determined to be $\langle\beta^2\rangle^{1/2} = 0.099$ and 0.112, respectively. So, a deformation $\langle\beta^2\rangle^{1/2} \sim 0.12$ is expected for the ^{189}Tl ground state. The comparison of the part d of the level scheme and the theoretical predictions shown in fig. 10 for $|\beta| \sim 0.12$ suggests that the low-spin part of ^{189}Tl might rather correspond to a prolate nuclear shape. The

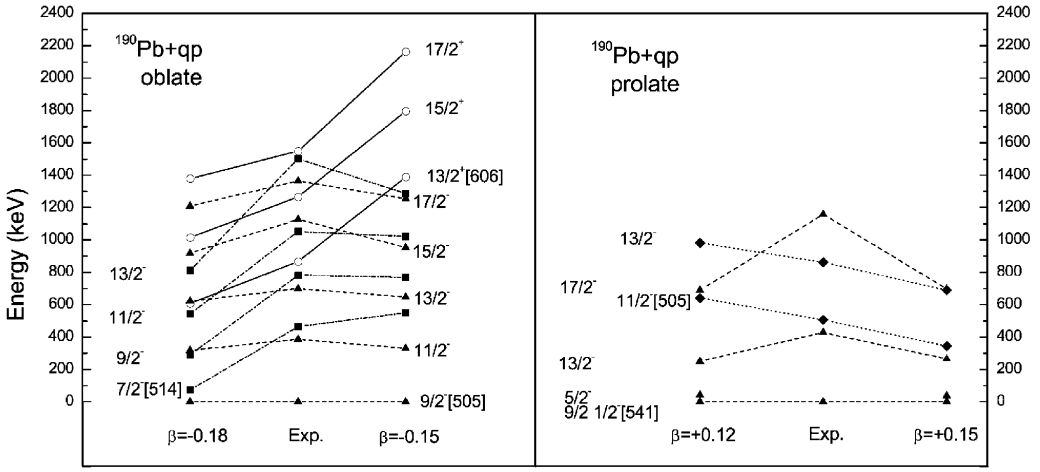

Fig. 11. Comparison, in the framework of the proposed identifications, of the experimental levels with the theoretical predictions obtained using the ^{190}Pb core with $\beta = -0.18$ and $\beta = -0.15$ for the oblate nuclear shape (left panel) and $\beta = +0.12$ and $\beta = +0.15$ for the prolate nuclear shape (right panel).

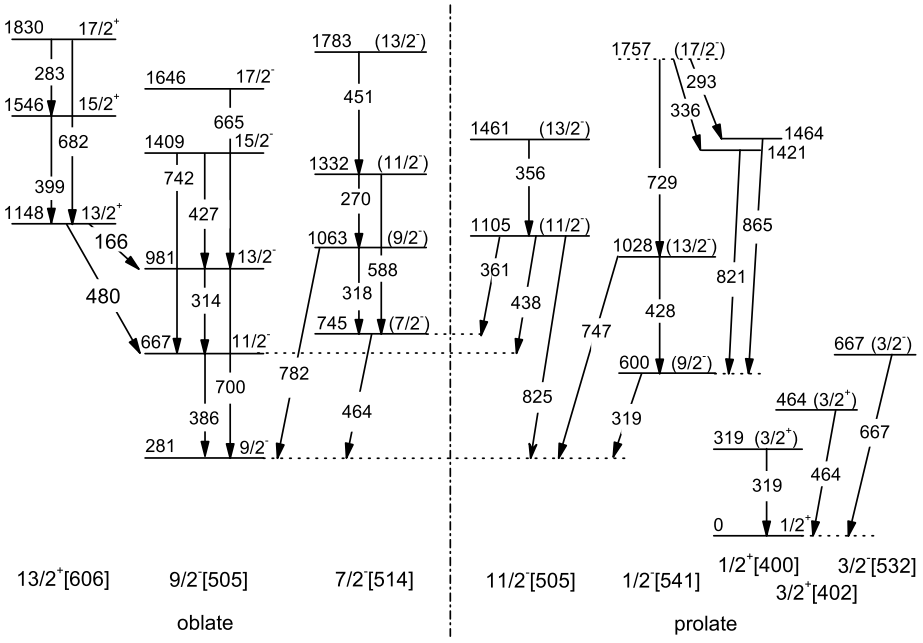

Fig. 12. Levels of the ^{189}Tl level scheme for which a structure has been proposed.

experimental level density observed below 1 MeV is indeed better reproduced assuming a prolate nuclear shape than assuming an oblate nuclear shape. The $1/2^+$ ground state would have then as main component of the wave function, the $1/2^+[400]$ state, and the 318.8, 463.7 and 667.4 keV levels would have the $3/2$ $1/2^+[400]$, $3/2^+[402]$ and $3/2^-[532]$ states as main components of their wave functions, respectively. However, given the scarcity of the experimental information in part *d* of the level scheme, it must be considered as tentative.

Finally, to summarize we show in fig. 12 the states of the ^{189}Tl level scheme for which a structure has been proposed. They are drawn as quasirotational bands labelled with the quantum numbers of the main component of the wave function describing the bandhead and the corresponding shape of the core. The theoretical approach allowed us to propose a structure to 20 levels among the 36 ones established below 1.8 MeV.

5 Conclusions

A level scheme of the ^{189}Tl nucleus has been established from the β^+/EC decay study of the ^{189}Pb isomers using both nuclear spectroscopy and in-source laser spectroscopy experiments. The hyperfine spectra obtained from gates set on main γ-rays have provided information on the feeding origin of the levels the γ-rays de-excite. For example, they clearly indicate that most of the levels shown in the parts *a*, *b* and *c* of the level scheme are purely fed from the ^{189}Pb high-spin isomer. Thus, the hyperfine spectra strongly suggest that parts *a*, *b* and *c* of the

level scheme are based on the isomeric level. The hyperfine spectra were essential to build the ^{189}Tl level scheme.

Calculations have been performed, for different oblate and prolate deformations, using the axial-rotor plus the one-quasiparticle coupling model. The theoretical predictions obtained in this way reproduced the experimental results concerning the levels previously identified; namely the states of the $9/2^-[505]$ and $13/2^+[606]$ bands corresponding to an oblate nuclear deformation with $\beta \sim -0.17$. Therefore, we have used the predictions provided by this model to propose a configuration for some other high-spin levels, namely states of the $7/2^-[514]$ band for an oblate nuclear shape and $11/2^-[505]$ and $9/2\ 1/2^-[541]$ bands for a prolate nuclear shape. To confirm these proposed identifications more experimental information is needed and, in particular, internal conversion coefficients that would provide transition multipolarities and would be able to confirm the spin and parity values of the excited states of the ^{189}Tl nucleus.

We would like to thank the ISOLDE collaborators for their technical assistance and cooperation. We are grateful to Dr. Ph. Dessagne and G. Heitz for technical help in the course of the experiment. We thank also the EURONS RII3-CT-2004-506065 project for granting access for some of us to ISOLDE via its funding for large-scale facilities. The support from the Federal Office for Scientific, Technical and Cultural Affairs (BriX-IAP P6/23 Program) and FWO-Vlaanderen (Belgium) is acknowledged.

References

1. H.-J. Kluge, W. Nörtershäuser, Spectrochim. Acta B **58**, 1031 (2003).
2. G. Ulm *et al.*, Z. Phys. A **325**, 247 (1986) and references therein.
3. T. Hilberath *et al.*, Z. Phys. A **342**, 1 (1992).
4. F. Le Blanc *et al.*, Phys. Rev. C **60**, 054310 (1999).
5. J. Sauvage *et al.*, Hyperfine Interact. **129**, 303 (2000).
6. V.S. Letokhov, V.I. Mishin, in *Laser Spectroscopy VIII*, edited by W. Persson, S. Svanberg, Springer Ser. Opt. Sci., Vol. **55**, 167 (1987).
7. J.A. Bounds *et al.*, Phys. Rev. C **36**, 2560 (1987).
8. R. Menges *et al.*, Z. Phys. A **341**, 475 (1992).
9. K. Wallmeroth *et al.*, Nucl. Phys. A **493**, 224 (1989).
10. G. Savard *et al.*, Nucl. Phys. A **512**, 241 (1990).
11. D. Verney *et al.*, Eur. Phys. J. A **30**, 489 (2006).
12. J.L. Wood, K. Heyde, W. Nazarewicz, M. Huyse, P. Van Duppen, Phys. Rep. **215**, 101 (1992).
13. K. Heyde, P. Van Isacker, M. Waroquier, J.L. Wood, R.A. Meyer, Phys. Rep. **102**, 291 (1983).
14. V. Berg, R. Foucher, Å. Höglund, the ISOLDE Collaboration, Nucl. Phys. A **244**, 462 (1975).
15. M.A. Deleplanque, C. Gerschel, N. Perrin, V. Berg, Nucl. Phys. A **249**, 366 (1975).
16. M.G. Desthuilliers *et al.*, Nucl. Phys. A **313**, 221 (1979).
17. C. Bourgeois, P. Kilcher, B. Roussière, J. Sauvage-Letessier, M.G. Porquet, the ISOCELE Collaboration, Nucl. Phys. A **386**, 308 (1982).
18. R. Béraud *et al.*, Nucl. Phys. A **284**, 221 (1977).
19. J.D. Cole *et al.*, Phys. Rev. C **16**, 2010 (1977).
20. W.C. Ma *et al.*, Phys. Lett. B **167**, 277 (1986).
21. J.P. Delaroche *et al.*, Phys. Rev. C **50**, 2332 (1994) and references therein.
22. A.N. Andreyev *et al.*, Nature **405**, 430 (2000).
23. J. Heese *et al.*, Phys. Lett. B **302**, 390 (1993).
24. J.F.C. Cocks *et al.*, Eur. Phys. J. A **3**, 17 (1998).
25. G.D. Dracoulis *et al.*, Phys. Lett. B **432**, 37 (1998).
26. D.J. Jenkins *et al.*, Phys. Rev. C **62**, 021302R (2000).
27. G.D. Dracoulis *et al.*, Phys. Rev. C **69**, 054318 (2004).
28. J. Pakarinen *et al.*, Phys. Rev. C **75**, 014302 (2007).
29. T. Grahn *et al.*, Phys. Rev. Lett. **97**, 062501 (2006).
30. M. Anselment *et al.*, Nucl. Phys. A **451**, 471 (1986) and references therein.
31. S.B. Dutta *et al.*, Z. Phys. A **341**, 39 (1991) and references therein.
32. H. De Witte *et al.*, Phys. Rev. Lett. **98**, 112502 (2007).
33. J.L. Wood, G.M. Gowdy, L.L. Riedinger, E.F. Zganjar, J.D. Cole, Jahresbericht GSI Darmstadt **58** (1979).
34. L.L Riedinger *et al.*, *Proceedings of the Workshop Gammasphere Physics* (World Scientific, Singapore, 1996) p. 98.
35. M. Seliverstov *et al.*, in preparation.
36. M. Meyer, J. Danière, J. Letessier, P. Quentin, Nucl. Phys. A **316**, 93 (1979).
37. E. Kugler *et al.*, Nucl. Instrum. Methods B **70**, 41 (1992).
38. J. Lettry *et al.*, Rev. Sci. Instrum. **69**, 761 (1998).
39. U. Köster *et al.*, Nucl. Instrum. Methods B **204**, 347 (2003).
40. A.N. Andreyev *et al.*, Eur. Phys. J. A **14**, 63 (2002).
41. R. Dissert, H. Friedmann, M. Klipfel, A. Krauth, R. Limbach, G. Walter, CRN report (1990), ISBN 0755-3404, p. 156.
42. S. Du, O. Hubert, J. Le Bris, R. Sellem, IPNO Report (1998-1999) Technical Activities, p. 110; J. Le Bris *et al.*, Rapport interne IPNO 06-03 (English version), IPNO 05-04 (French version).
43. M.-G. Porquet *et al.*, Phys. Rev. C **44**, 2445 (1991) and references therein.
44. W. Reviol *et al.*, Phys. Scr. T **56**, 167 (1995).
45. G.M. Gowdy, PhD Thesis, Georgia Institute of Technology (1976).
46. E. Coenen, K. Deneffe, M. Huyse, P. Van Duppen, J.L. Wood, Phys. Rev. Lett. **54**, 1783 (1985).
47. H. Dautet, private communication.
48. J.B. Niday, R. Gummick, *Computerized quantative analysis by γ-ray spectrometry*, Vol. **III**, *A user's guide to Gamanal*, University of California, LLNL Report UCRL-51061, Vol. **1** (1972).
49. J.F. Rabasse, SlabView 1.3 User's Manual IPNO, S2I (1998).
50. A.J. Kreiner *et al.*, Phys. Rev. C **38**, 2674 (1988).
51. Band-Raman, Internal Conversion Coefficients, `http://www.nndc.bnl.gov/bricc/`.
52. N.B. Gove, M.J. Martin, Nucl. Data A **10**, 205 (1971).
53. `http://www.nndc.bnl.gov/chart/chartNuc.jsp`.
54. S. Franchoo *et al.*, IPNO-DR Annual report (2004-2005) p. 6; J. Genevey *et al.*, LPSC Annual report (2004-2005) p. 55.
55. S. Raman, N.B. Gove, Phys. Rev. C **7**, 1995 (1973).
56. T. Awaya, Nucl. Instrum. Methods **174**, 237 (1980).
57. D. Vautherin, D.M. Brink, Phys. Rev. C **5**, 626 (1972).
58. D. Vautherin, Phys. Rev. C **7**, 296 (1973).
59. H. Flocard, P. Quentin, A.K. Kerman, D. Vautherin, Nucl. Phys. A **203**, 433 (1973).
60. M. Beiner, H. Flocard, Nguyen Van Giai, P. Quentin, Nucl. Phys. A **238**, 29 (1975).